SUPPLEMENTAL TABLES

Supplemental Table 1. Human TCR complex deficiencies [A]

				References		Number of patients	
Protein	**Gene**	**Chr.**	**OMIM**	**Complete**	**Leaky**	**Complete**	**Leaky**
CD3γ	*CD3G*	11	186740	1		5	
CD3δ	*CD3D*	11	186790	2,3,4	[B]	7	2 [B]
CD3ε	*CD3E*	11	186830	3	5	3	1
TCRζ	*CD247*	1	186780	6	7	1	1
TCRα	*TRAC* [C]	14	186880	8		2	
					Total	**18**	**4**

[A] Classified as complete or leaky according to the effect of the mutations. Leaky, but not complete, mutations allow for the synthesis of low amounts of the wild type protein.
[B] Present manuscript. The GenBank accession no. for the cDNA and genomic DNA mutant sequences are JN392069 and JN392070, respectively.
[C] TCRα constant gene segment.

Supplemental Table 2. Primers used for RT-PCR [A]

Gene	Primer	Sequence (5´ to 3´)
CD3G	CD3GF	AAAAAGAATTCTCAATTCCTCCTCAACTC
	CD3GR	AAAAAGGATCCATGGAACAGGGGAAGGG
CD3D	CD3DF	CTGTAGGAATTCACGATGGAACATAGCACGTTTCTC
	CD3DR	CTAGCTCTCGAGTCACTTGTTCCGAGCCCAGTT
CD3E	CD3EF	TTCCTGTGTGGGGTTCAGAAACC
	CD3ER	CCATCAGGCTGAGGAACGATTCT
CD247	CD247F	CTGAGGGAAAGGACAAGATGAAG
	CD247R	AAAGAGTGCAGGGACAACAGTCT

[A] OLIGO Primer Analysis Software version 7 from Molecular Biology Insights was run for the following gene sequences (GenBank accession no.): *CD3G* (NM_000073), *CD3D* (NM_000732), *CD3E* (NM_000733) and *CD247* (NM_0007343.3).

Supplemental Table 3. Primers used for genomic PCR (exons+flanking introns) [A]

Gene	Exon	Sequence (5´ to 3´)	
		Forward	Reverse
CD3D	1	AGCTCTCACCCAGGCTGATAGT	AAGCTCTGGGATTACTGGTGTGA
	2	TGAGCTTCCGCAGAACAAAGG	CACATCCAGAAGCCCTATCCATT
	3	AGGATGGTTCCCTGATCTTAAAGG	CACTCTCATGCTCTGCTCTTCCA
	4-5	GGTGGATCTCACAGTCCCATCT	TATATTTATTGGCTGAGCAAGAAGG

[A] OLIGO Primer Analysis Software version 7 from Molecular Biology Insights was run for *CD3D* (NG_009891.1)

Supplemental Table 4. Primers and probes used for quantitative PCR [A]

Gene	Primer/Probe	Sequence (5´ to 3´)
CD3DWT	Forward	AGGACAAAGAATCTACCGTGCAA
	Reverse	CACGGTGGCTGGATCCA
	Probe	ATTATCGAATGTGCCAGAGC
CD3DΔEx2	Forward	CGTTTCTCTCTGGCCTGGTACT
	Reverse	CACGGTGGCTGGATCCA
	Probe	ACCCTTCTCTCGCAAGTGTGCCAGA
CD3E	Forward	CAAGGCCAAGCCTGTGAC
	Reverse	TCATAGTCTGGGTTGGGAACA
	Probe	49 (Universal ProbeLibrary for Human, Roche)

[A] Primer Express 3.0 from Applied Biosystems was used for *CD3DWT* and *CD3DΔEx2*, and ProbeFinder version 2.40 for Human (Universal ProbeLibrary Assay Design Center) from Roche Applied Science was used for *CD3E*. Sequences as in Supplemental Table 2.

SUPPLEMENTAL METHODS

The S2 *Drosophila* cell reconstitution system

Schneider S2 cells were grown in Schneider's *Drosophila* medium and transfected using CellFectin (Invitrogen Life Technologies) as described (9). Expression vectors for CD3ε, CD3γ and TCRζ were generated as described (10) and for TCRα, TCRβ, CD3δ, ΔEx2 and ΔEx3 is explained below. After 24 h, protein expression was induced by addition of 1mM $CuSO_4$ for another 20 h. Subsequently, cells were either stained for flow cytometry or lysed as described (9, 10). For IP 3 μg of antibody and 5 μl of protein G-coupled Sepharose (GE Healthcare) was incubated with 300 μl of cell lysate overnight at 4°C. Beads were washed 3 times in lysis buffer before standard SDS-PAGE and Western blotting.

Generation of *Drosophila* expression vectors

The cDNAs of the proteins of interest were inserted into the Drosophila expression vector pRmHa-3 containing an inducible metallothionein promotorer (11). pRmHa-3 is abbreviated as pD. The coding sequences of human WT CD3δ, ΔEx2 and ΔEx3 were cloned into the pD vector using EcoRI and XhoI restriction sites from the pIREShrGFPCD3DWT, pIREShrGFPCD3DΔExon2 and pIREShrGFPCD3DΔExon3 plasmids. ΔEx3 CD3δ lacks the transmembrane region and is associated with severe αβ and γδ T lymphopenia and SCID (4). pDECFPhTCRαHA1.7 and pDECFPhTCRβ HA1.7, containing sequences that encode for an N-terminally ECFP-tagged HA-specific human TCRα or TCRβ chain, were derived from the plasmids pJ6omegaTCRαHA1.7 or pJ6omegaTCRβHA1.7, respectively.

Reconstruction of the TCR complex in *Drosophila* S2 cells

To study TCR assembly, we used the S2 *Drosophila* cell reconstitution system that allows co-transfection and expression of more than 5 different vectors (12). We had used this system previously to reconstruct assembly and surface transport of the BCR complex (13). Here, we firstly show that TCRαβ dimers do not come to the S2 cell surface if expressed alone, whereas CD3εδ and CD3εγ do (Supplemental Figure 4A). Co-expression of a CD3 dimer together with TCRαβ leads to surface expression of TCRαβ, showing that some aspects of TCR assembly and transport to the surface can

be studied using this system (Supplemental Figure 4B). Next, S2 cells were co-transfected with plasmids containing cDNAs of WT CD3ε and WT CD3δ or ΔEx2 or ΔEx3. CD3 proteins were IP from the lysates with a mAb specific for folded CD3ε (OKT3) and a CD3δ-specific antiserum (M20δ), separated by non-reducing SDS-PAGE and detected by CD3δ- or CD3ε-specific antisera by Western blotting (Supplemental Figure 4C). ΔEx2, but not ΔEx3, gave rise to a stable protein (bottom left panel) which was able to pair with CD3ε (bottom right panel). The smallest ΔEx2 form might be a disulphide-linked dimer of nearly the same size as a WT CD3δ monomer. CD3ε of the ΔEx2-CD3ε dimers was not folded correctly, since it was not recognized by OKT3 (upper panels), and was aberrantly disulphide bonded to ΔEx2 (lower left panel). Only WT CD3δ produced CD3δε dimers that were recognized by IP using the mAb OKT3 (upper panels) and by flow cytometry using UCHT1 (Supplemental Figure 4D). Furthermore, ΔEx2 could not diminish expression of a TCR complex (Supplemental Figure 4E), although it was expressed at higher levels than WT CD3δ (Supplemental Figure 4C bottom left). Therefore, the head-less CD3δ did not efficiently compete with WT CD3δ in the formation of a TCR complex. From these results we concluded that ΔEx2 was unlikely to impinge on αβTCR assembly or surface expression in the patients' T cells.

***TCRB* clonality**

Clonality at the *TCRB* locus was studied using a commercial kit (Master Diagnostica, Granada, Spain, EC-certified for clinical use), which amplifies genomic TCR VβJβ rearrangements using two primers specific for conserved V and J flanking regions. Polyclonal (normal donor) and monoclonal (Jurkat or MOLT3) control DNAs were included for reference. Amplimers were separated and analyzed in an ABI Prism Genetic Analyzer 3110 using GeneMapper V 4.0 from ABI.

SUPPLEMENTAL FIGURES

Supplemental Figure 1. *CD3D* intron 2 5´ splice donor site phylogeny. Multiple alignment of DNA sequences of the gene region surrounding the IVS2+5G>A mutation (arrow) in several mammals (*hominids) reveals that the location of the mutation is conserved. The equivalent location after the exon encoding the extracellular Ig domain is also conserved as a guanine in *CD3G* (not shown).

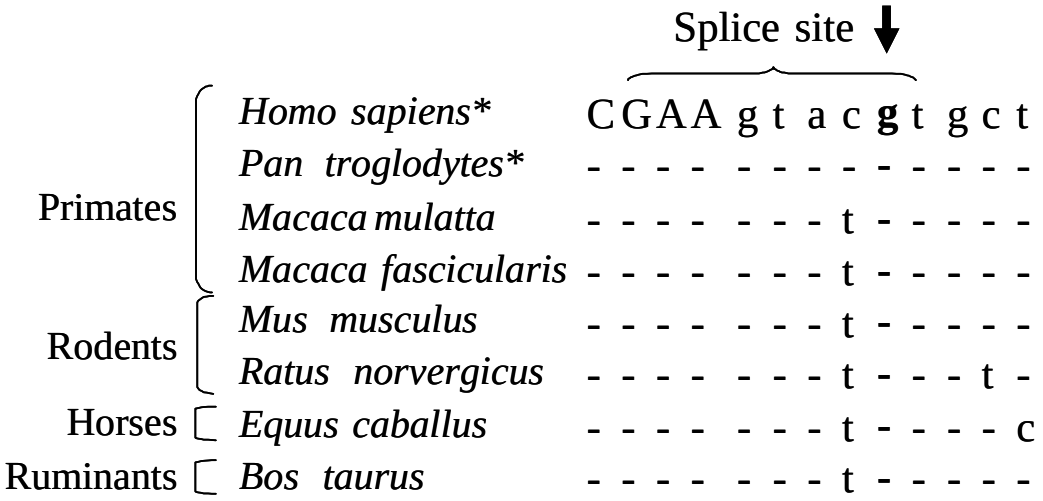

Supplemental Figure 2. Genetic pedigrees and *CD3* haplotype analysis. Genetic pedigrees of the two families with the *CD3D* mutation. Circles indicate females, squares indicate males (slashed when deceased). Solid symbols denote homozygosity for the mutation, half-solid symbols heterozygosity. *CD3* haplotypes under each symbol are based on the indicated polymorphic markers spanning the *CD3GDE* region on chromosome 11q23. The disease-associated chromosomes are depicted in black with the shared core haplotype markers in red. No genotyping inconsistencies were found. The relative order and the physical distances of markers are as previously reported (1). The allele sizes are normalized with respect to individual 134702, available from Center d'Etude du Polymorphisme Humain (14).

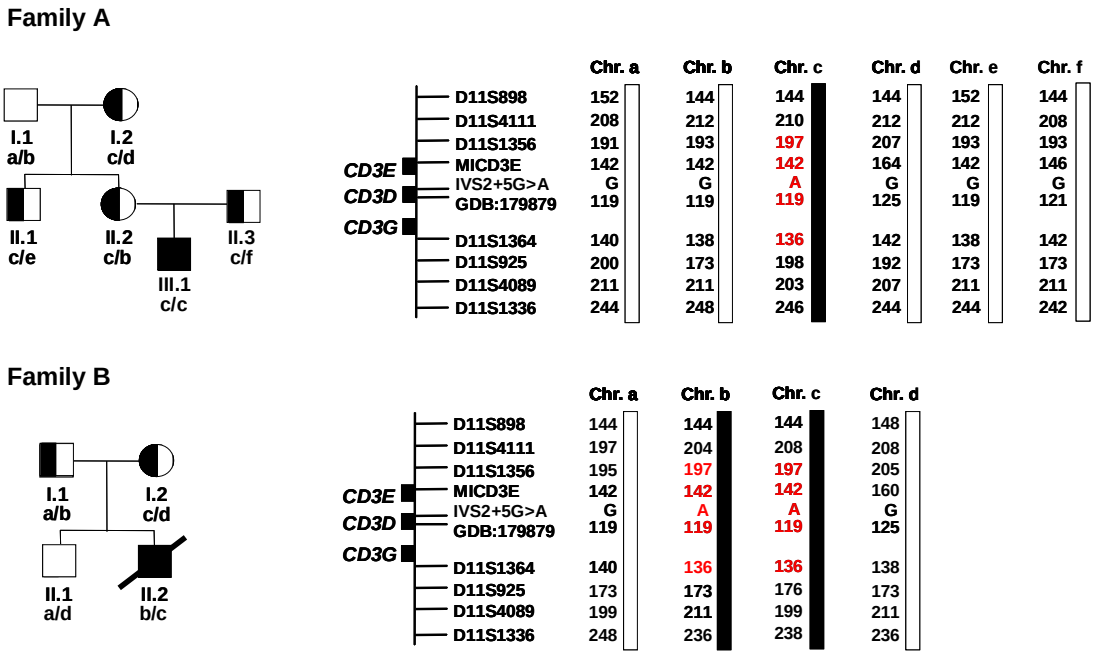

Supplemental Figure 3. TCR complex expression in cultured T cells from patients (dashed lines) or controls (solid lines). (A) Lymphocytes were fixed with 2% paraformaldehyde at $3x10^6$ cells/ml for 1 hour at 4ºC, permeabilized using 0.2% saponin for 15 minutes at room temperature and stained with APA1/2 (anti-human CD3δ cytoplasmic tail mAb, 15) followed by anti-mouse IgG-PE (Beckman Coulter). WT Jurkat cells were compared with CD3δ knock-down (KD) cells using a specific shRNA for CD3δ RNA which showed a 90% reduction in CD3δ by Western blotting (right, shCD3δ 3). The numbers in each histogram indicate the MFI ratios between control and patient or KD. **(B)** Lymphocytes were surface-stained with the indicated TCR- or CD3-specific mAb and analyzed comparatively within the indicated gates. Tαβ cells were defined as $BMA031^+$, $CD3^+IMMU510^-$ or $WT31^+$, whereas Tγδ cells were defined as $IMMU510^+$. Histogram numbers as in A.

A Intracellular CD3δ expression

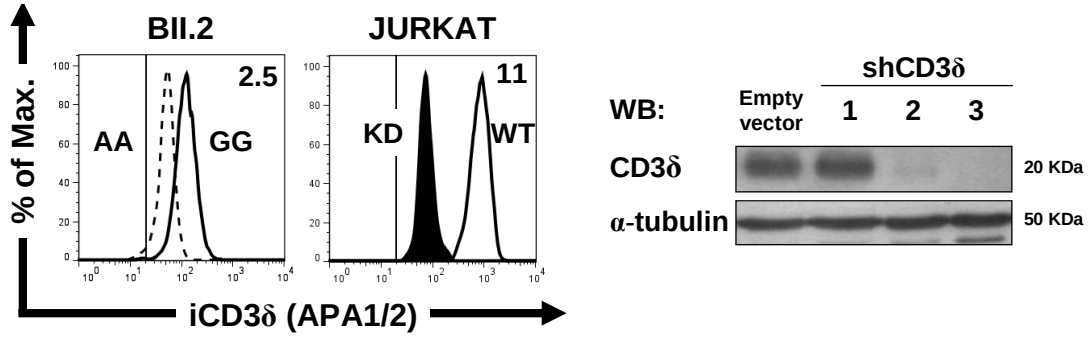

B Surface expression

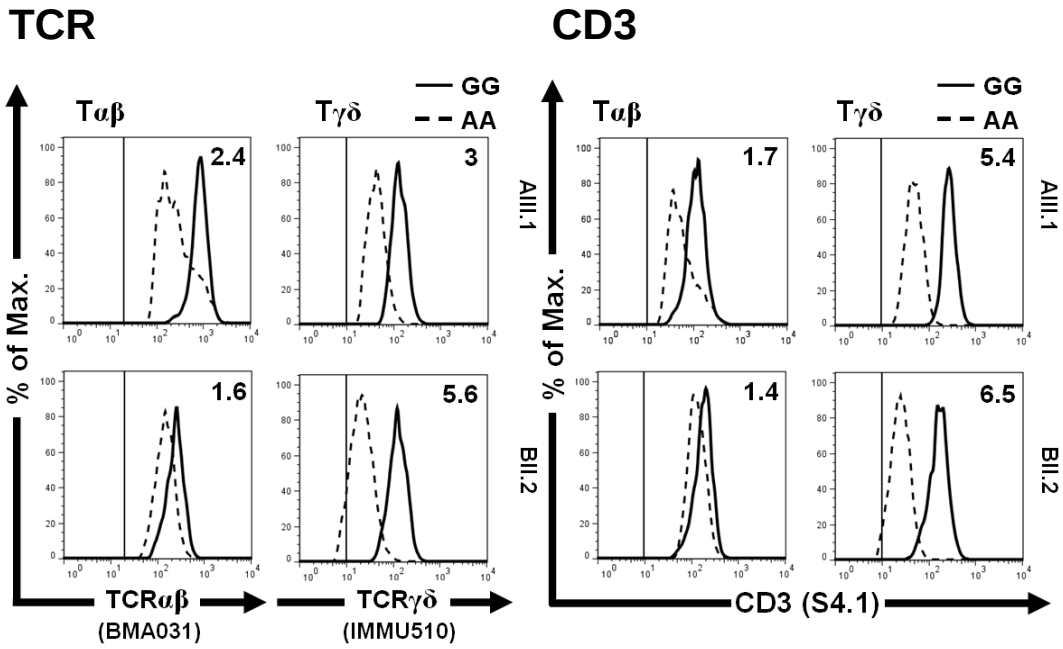

Supplemental Figure 4. Reconstruction of the TCR complex in *Drosophila* S2 cells (A, B, C) to show that ΔEx2 does not compete with WT CD3δ to form a TCR complex (D, E). Refer to Supplemental Methods for details.

(A) *Drosophila* S2 cells were transiently transfected with expression plasmids encoding for the indicated proteins or with the empty plasmid (-). After induction with copper sulfate, cells were stained first extracellularly and then after permeabilisation with saponin intracellularly with anti-TCRβ (Jovi1, left panels) or anti-folded CD3ε (UCHT1, right panel) antibodies and measured by flow cytometry. **(B)** Summary of the expression of TCRαβ (column "αβ") or CD3 (column "ε") on the *Drosophila* S2 cell surface after co-expression of the TCR or CD3 subunits indicated in the left column. Experiments were done as in A) using mouse or human expression plasmids as indicated. - : no expression on the cell surface; + : low and ++ : high expression on the cell surface. As a control, all human TCR and CD3 subunits were expressed as seen by Western blotting (data not shown). Co-expression of a CD3 dimer together with TCRαβ leads to surface expression of TCRαβ, which was not enhanced upon transfection of all six TCR and CD3 subunits. **(C)** S2 *Drosophila* cells were transiently transfected with expression plasmids encoding for the indicated proteins (lanes 1-4 and 6) or with the empty plasmid (lane 5). After induction with copper sulfate, the lysates (lowest panel) or anti-folded CD3ε or anti-CD3δ IP (OKT3, upper panels, or M20δ, lower panels, respectively) were separated by non-reducing SDS-PAGE. Western blotting was performed with anti-CD3δ (M20δ, left panels) or anti-CD3ε (M20ε, right panels) antibodies and the ECL system. **(D)** S2 cells were transiently transfected with expression plasmids encoding for the indicated proteins. After induction with copper sulfate, cells were stained with the anti-TCRβ antibody Jovi3 and measured by flow cytometry. **(E)** S2 cells were transiently transfected with expression plasmids encoding for the indicated proteins (coloured lines) or with the empty plasmid (black lines). After induction with copper sulfate, cells were stained with the anti-folded CD3ε antibody UCHT1 and measured by flow cytometry.

A

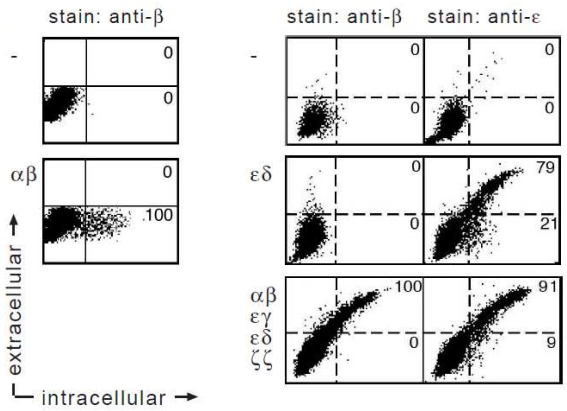

B

co-expression	mouse αβ	mouse ε	human αβ	human ε
αβ	-		-	
εγ		++		++
εδ		++		++
αβ ε	-		-	
αβ γ	-		-	
αβ δ	-		-	
αβ εγ	++	++	+	+
αβ εδ	++	++	++	++
αβ ζζ	-		-	
αβ εγ εδ	++	++	++	++
αβ εγ εδ ζζ	++	++	++	++

C

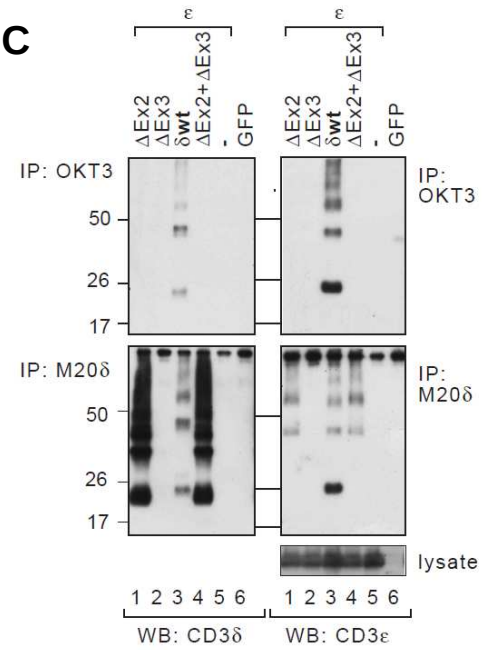

D

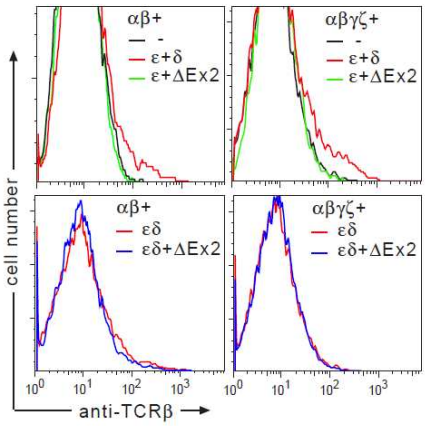

E

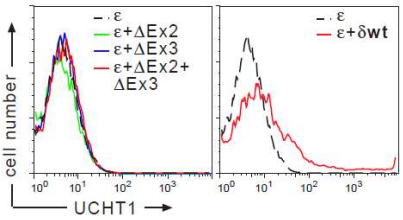

Supplemental Figure 5. Tαβ lymphocyte subset numbers. Absolute $CD4^+$ and $CD8^{bright}$ cell numbers in patients (AIII.1 dots, BII.2 triangles) plotted as a function of age in comparison with the normal age-matched distribution (P5, P50 and P95, 16).

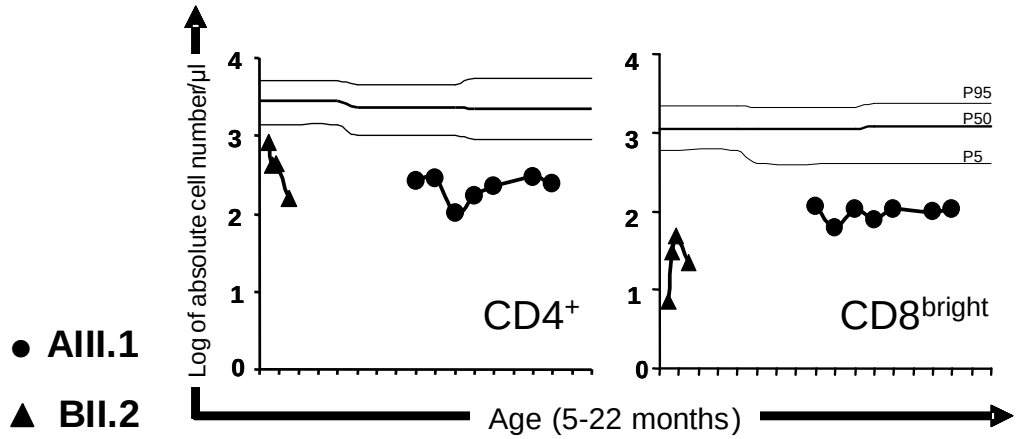

Supplemental Figure 6. TCR complex function. (A) TCR down-regulation after 24 hours in response to anti-CD3 stimulation in primary Tαβ ($CD4^+$) or Tγδ ($11F2^+$) lymphocytes with the indicated *CD3D* IVS2+5 genotypes. The numbers in each histogram indicate CD3 MFI percentages of stimulated (dashed lines) relative to unstimulated cells (solid lines). **(B)** CD69 induction (% expression) in T cell lines from the indicated donors after stimulation with different amounts of UCHT-1 for 24 hours. **(C)** CD25 induction after 36 hours in stimulated (dashed lines) compared to unstimulated (solid lines) primary $CD4^+$ T cells (moslty Tαβ cells). The numbers in each histogram indicate MFI increments normalized to control cell increments. **(D)** Lymphocyte proliferation was evaluated by flow cytometry using CFSE dye dilution (17). CFSE-labeled peripheral blood lymphocytes were cultured for 5 days in the presence (+) or absence (─) of phytohemagglutinin (PHA, left) or the anti-CD3 antibody UCHT-1 (right). Cells were analyzed for CFSE dilution by flow cytometry within the indicated subsets. In this experiment Tαβ and Tγδ lymphocytes were defined as $CD4^+$ (>98% Tαβ cells), and double negative $CD3^+$ (78±6% Tγδ cells) because the TCR was down-regulated after activation.

A TCR down-regulation

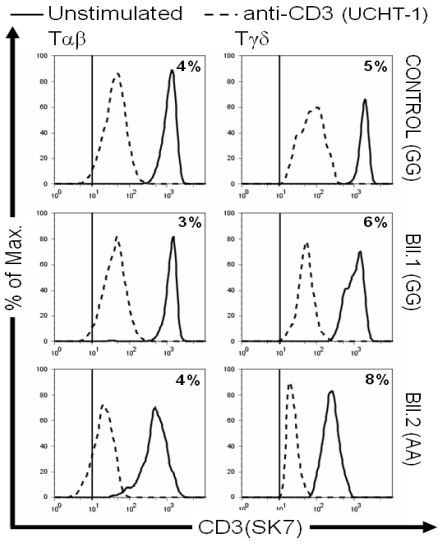

B CD69 induction

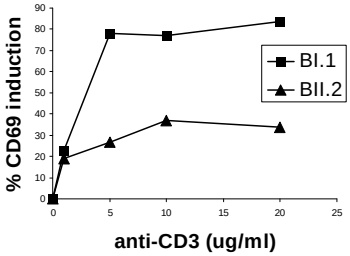

C CD25 induction

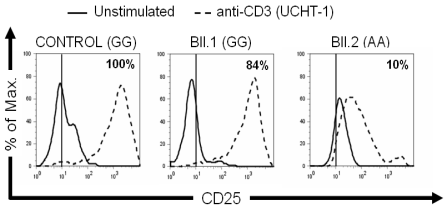

D Lymphocyte proliferation

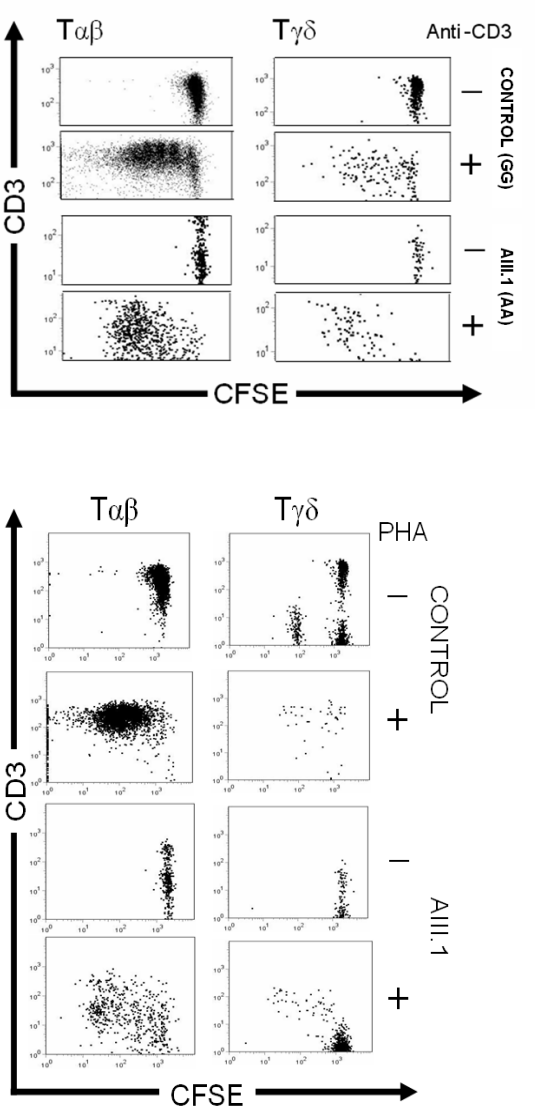

Supplemental Figure 7. Thymus of patient AIII.1 at diagnosis (chest CT scan). Patient AIII.1 showed a thymus of 2.39 x 1.8 cm (1 and 2 in image, respectively), within the normal age-matched dimensions ± SD of 3.13 ± 0.85 x 2.52 ± 0.82 (18). In patient BII.2 the thymus was initially not detected by CT scan, but his necropsy revealed the presence of a thymus remnant of 2 x 1 cm.

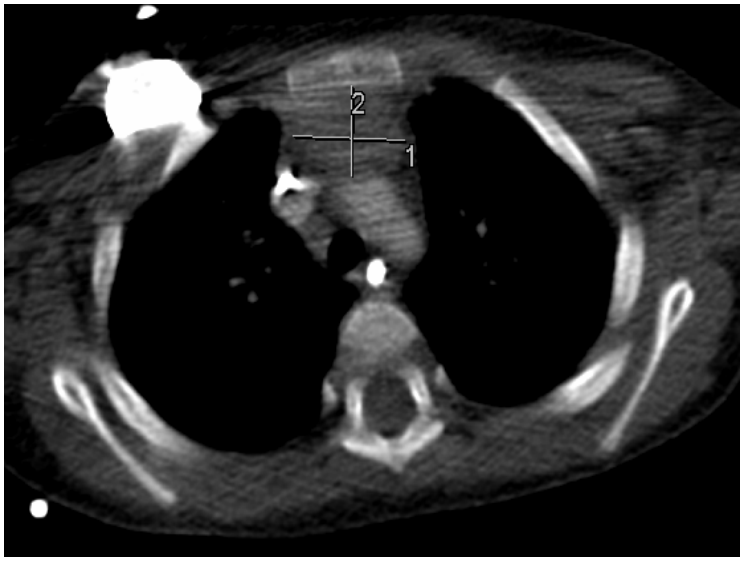

Supplemental Figure 8. T lymphocyte phenotype in the patients to a normal age-matched control. (A) Recent thymic emigrants defined as $CD4^+CD45RA^+CD31^+$ T cells (19). **(B)** $CD45RA^+$ (naïve) and $CD45RO^+$ (memory) T lymphocytes. **(C)** CD25 expression in patients with *CD3D* IVS2+5 AA genotype (dashed lines) in comparison with controls (GG, solid lines) in Tαβ cells defined as $CD4^+$ and in Tγδ cells defined as $11F2^+$.

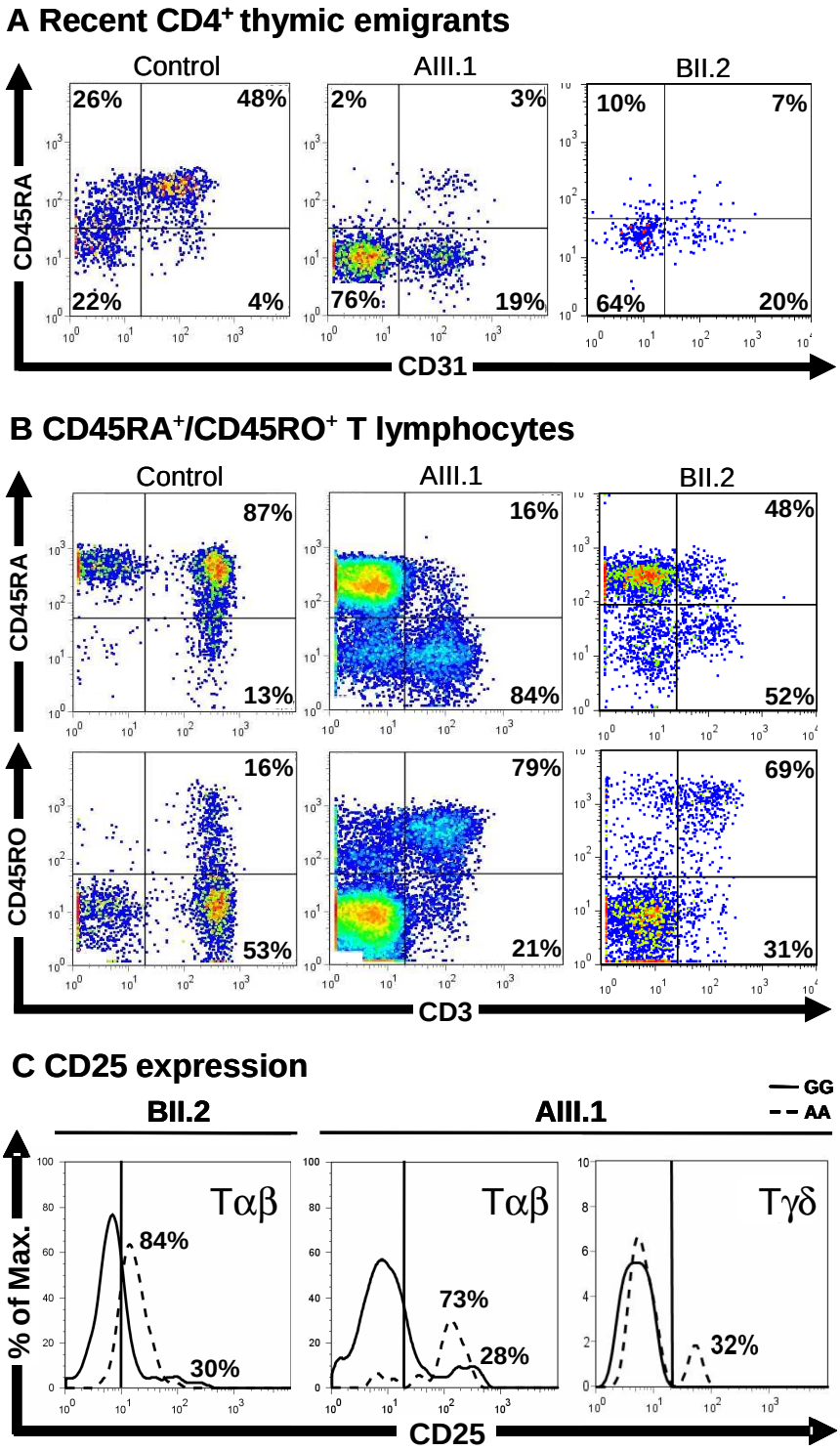

Supplemental Figure 9A. *TCRB* clonality. Genomic *TCR VβJβ* rearrangements were amplified in the patients using two different primer sets (VBJB-A and –B) and compared with a normal (polyclonal) donor and two tumoral T cell lines (monoclonal) in the 240-280 bp range. The two primer sets are specific for conserved V and J flanking regions, and therefore amplify genomic *TCR VβJβ* rearrangements as fragments of the indicated size range (see Supplemental Methods in page 4). Normal T lymphocytes are polyclonal and thus show a Gaussian fragment distribution (POLYCLONAL in Figure). T lymphoid tumors such as Jurkat or MOLT3 are monoclonal and thus yield a single major peak (MONOCLONAL in Figure). Patients with poor TCRβ diversity show few peaks without Gaussian distribution.

A *TCRB* clonality

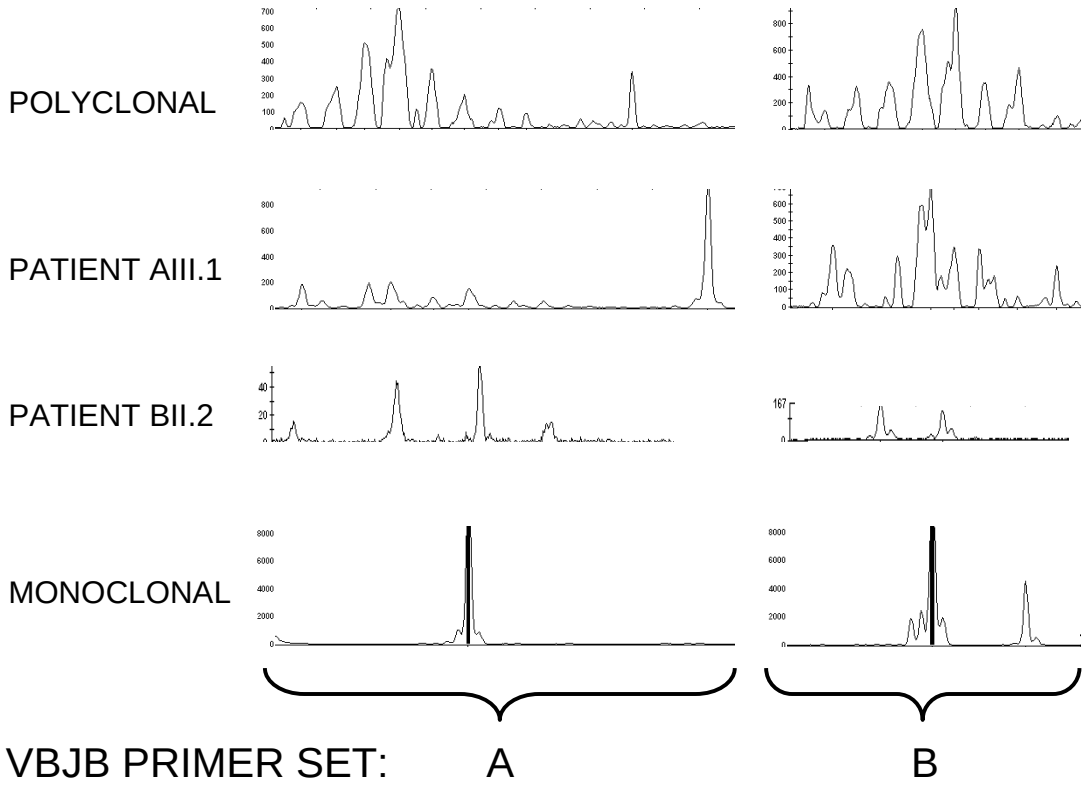

Supplemental Figure 9B. TCRVβ repertoire within $CD4^+$ and $CD8^+$ T populations by flow cytometry using a collection of anti-TCR Vβ antibodies from Beckman Coulter Immunotech. Data are shown within range (green) or out of range (red) (black, not done) in comparison with a normal age-matched control (empty bars) and the normal range (grey bars ± SD, 20).

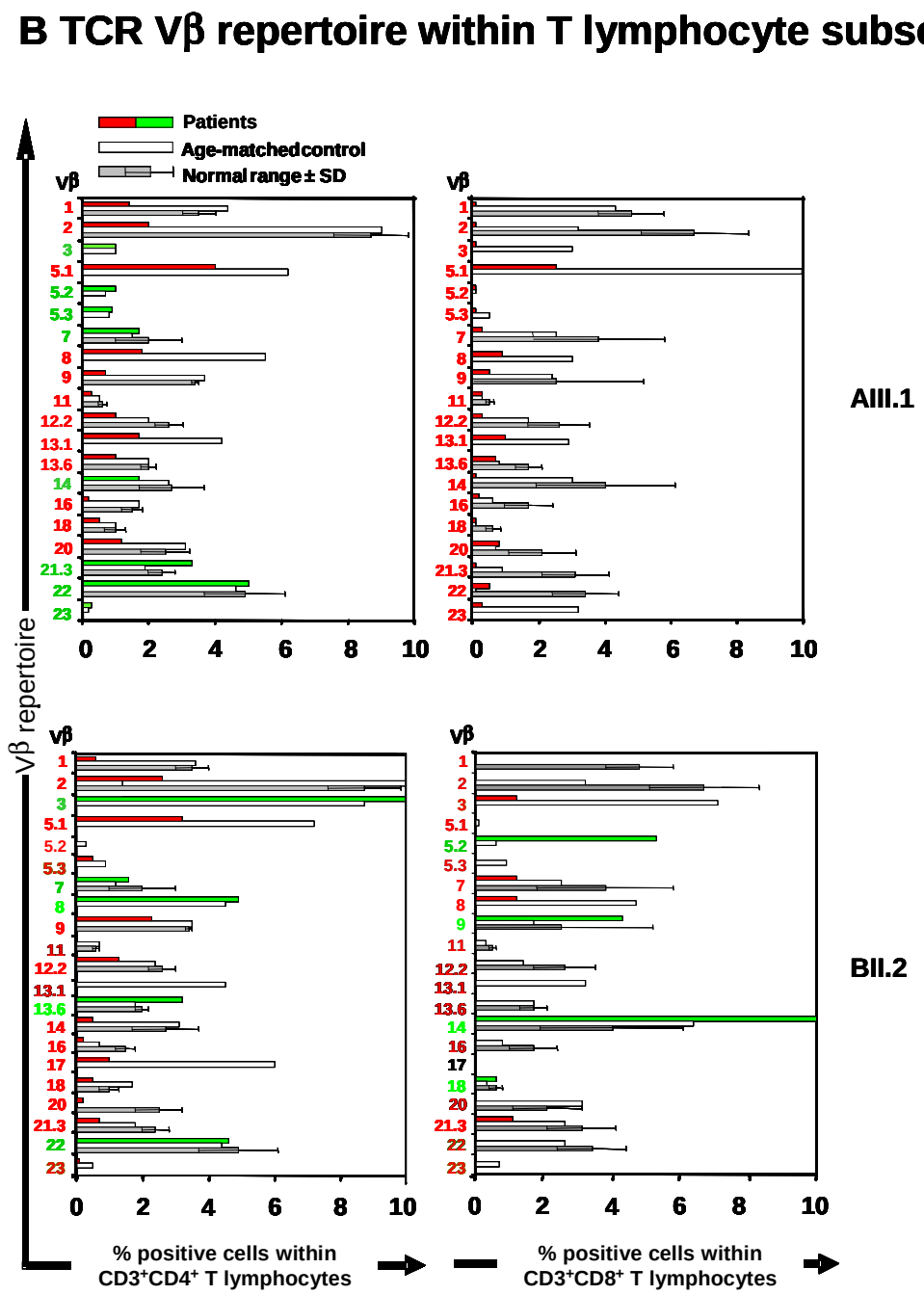

SUPPLEMENTAL REFERENCES

1. Recio MJ, et al. Differential biological role of CD3 chains revealed by human immunodeficiencies. *J Immunol.* 2007;178(4):2556-64.
2. Dadi HK, Simon AJ, Roifman CM. Effect of CD3delta deficiency on maturation of alpha/beta and gamma/delta T-cell lineages in severe combined immunodeficiency. *N Engl J Med.* 2003;349(19):1821-28.
3. de Saint Basile G, et al. Severe combined immunodeficiency caused by deficiency in either the delta or the epsilon subunit of CD3. *J Clin Invest.* 2004; 114(10):1512-17.
4. Takada H, Nomura A, Roifman CM, Hara T. Severe combined immunodeficiency caused by a splicing abnormality of the CD3delta gene. *Eur J Pediatr.* 2005;164(5):311-14.
5. Soudais C, Villartay J P, Deist F L, Fischer A, Lisowska-Grospierre B. Independent mutations of the human CD3-epsilon gene resulting in a T cell receptor/CD3 complex immunodeficiency. Nat Genet 3:77-81, 1993
6. Roberts JL, et al. $T^{-}B^{+}NK^{+}$ severe combined immunodeficiency caused by complete deficiency of the CD3zeta subunit of the T-cell antigen receptor complex. *Blood*. 2007;109(8):3198-206.
7. Rieux-Laucat F, Hivroz C, Lim A, et al. Inherited and somatic CD3zeta mutations in a patient with T-cell deficiency. N Engl J Med 2006; 354: 1913-21.
8. Morgan NV, et al. Mutation in the TCRα subunit constant gene (TRAC) leads to a human immunodeficiency disorder characterized by a lack of TCRαβ+ T cells. *J Clin Invest.* 2011;121(2):695-702.
9. Swamy M, Kulathu Y, Ernst S, Reth M, Schamel WW. Two dimensional Blue Native-/SDS-PAGE analysis of SLP family adaptor protein complexes. *Immunol Lett.* 2006;104(1-2):131-7.
10. Dopfer EP, et al. Analysis of novel phospho-ITAM specific antibodies in a S2 reconstitution system for TCR-CD3 signalling. *Immunol Lett.* 2010;130(1-2):43-50.
11. Bunch TA, Grinblat Y, Goldstein LS. Characterization and use of the Drosophila metallothionein promoter in cultured Drosophila melanogaster cells. *Nucleic Acids Res.* 1988;16(3):1043-61.
12. Rolli V, et al. Amplification of B cell antigen receptor signaling by a Syk/ITAM

positive feedback loop. *Mol Cell.* 2002;10(5):1057-69.

13. Schamel WW, Kuppig S, Becker B, Gimborn K, Hauri HP, Reth, M. A high molecular weight complex of BAP29/BAP31 is involved in the retention of membrane-bound IgD in the endoplasmic reticulum. *Proc Natl Acad Sci.* 2003; 100(17):9861-66.
14. Dib C, et al. A comprehensive genetic map of the human genome based on 5,264 microsatellites. *Nature.* 1996;380(6570):152-4.
15. Alarcón A, et al. The CD3γ and CD3δ subunits of the T cell antigen receptor can be expressed within distinct funcional TCR/CD3 complex. *EMBO J.* 1991;10(4): 903-12.
16. Comans-Bitter WM, et al. Immunophenotyping of blood lymphocytes in childhood. Reference values for lymphocyte subpopulations. *J Pediatr.* 1997; 130(3):388-93.
17. Lyons AB. Analysing cell division in vivo and in vitro using flow cytometric measurement of CFSE dye dilution. *J Immunol Methods.* 2000;243(1-2):147-54.
18. Francis IR, Glazer GM, Bookstein FL, Gross BH. The thymus: Reexamination of age-related changes in size and shape. *AJR Am J Roentgenol.* 1985;145(2): 249-54.
19. Kohler S, Thiel A. Life after the thymus: $CD31^+$ and $CD31^-$ human naïve $CD4^+$ T-cell subsets. *Blood.* 2009;113(4):769-74.
20. van den Beemd R, et al. Flow Cytometric Analysis of the Vb Repertoire in Healthy Controls. *Cytometry.* 2000;40(4):336-45.